

# ADVANCED ENERGY MATERIALS

## Supporting Information

for *Adv. Energy Mater.*, DOI: 10.1002/aenm.201700099

Subtle Roles of Sb and S in Regulating the Thermoelectric Properties of N-Type PbTe to High Performance

*Gangjian Tan, Constantinos C. Stoumpos, Si Wang, Trevor P. Bailey, Li-Dong Zhao, Ctirad Uher, and Mercouri G. Kanatzidis\**

## Supporting Information

Subtle roles of Sb and S in regulating the thermoelectric properties of n-type PbTe to high performance

Gangjian Tan,<sup>1</sup> Constantinos C. Stoumpos,<sup>1</sup> Si Wang,<sup>2,3</sup> Trevor P. Bailey,<sup>2</sup>

Li-Dong Zhao,<sup>4</sup> Ctirad Uher,<sup>2</sup> and Mercuri G. Kanatzidis<sup>1\*</sup>

<sup>1</sup>Department of Chemistry, Northwestern University, Evanston, Illinois 60208, United States

<sup>2</sup>Department of Physics, University of Michigan, Ann Arbor, Michigan 48109, United States

<sup>3</sup>State Key Laboratory of Advanced Technology for Materials Synthesis and Processing, Wuhan University of Technology, Wuhan 430070, China

<sup>4</sup>School of Materials Science and Engineering, Beihang University, Beijing, 100191, China

\*Corresponding author: m-kanatzidis@northwestern.edu

Table S1. Densities of all the samples investigated in this study.

Compositions		Density ( $d$ , g/cm <sup>3</sup> )	Relative density* (%)
Pb <sub>1-x</sub> Bi <sub>x</sub> Te	x=0.3%	8.00	98.0
	x=0.5%	8.01	98.1
	x=0.7%	7.94	97.3
	x=1.0%	7.98	97.7
	x=1.25%	7.94	97.3
	x=1.5%	8.02	98.2
Pb <sub>1-x</sub> Sb <sub>x</sub> Te	x=0.3%	8.01	98.1
	x=0.5%	7.97	97.6
	x=0.7%	7.91	96.9
	x=1.0%	7.95	97.4
	x=1.25%	7.90	96.8
	x=1.5%	7.92	97.0
Pb <sub>0.9875</sub> Sb <sub>0.0125</sub> Te <sub>1-y</sub> S <sub>y</sub>	y=0.04	7.89	96.9
	y=0.08	7.87	96.8
	y=0.12	7.85	96.8
	y=0.16	7.83	96.7

\*The theoretical densities  $d(t)$  of the Pb<sub>1-x</sub>Bi<sub>x</sub>Te, Pb<sub>1-x</sub>Sb<sub>x</sub>Te, and Pb<sub>0.9875</sub>Sb<sub>0.0125</sub>Te<sub>1-y</sub>S<sub>y</sub> samples were calculated using the law of mixtures in light of the volume fraction of each component.

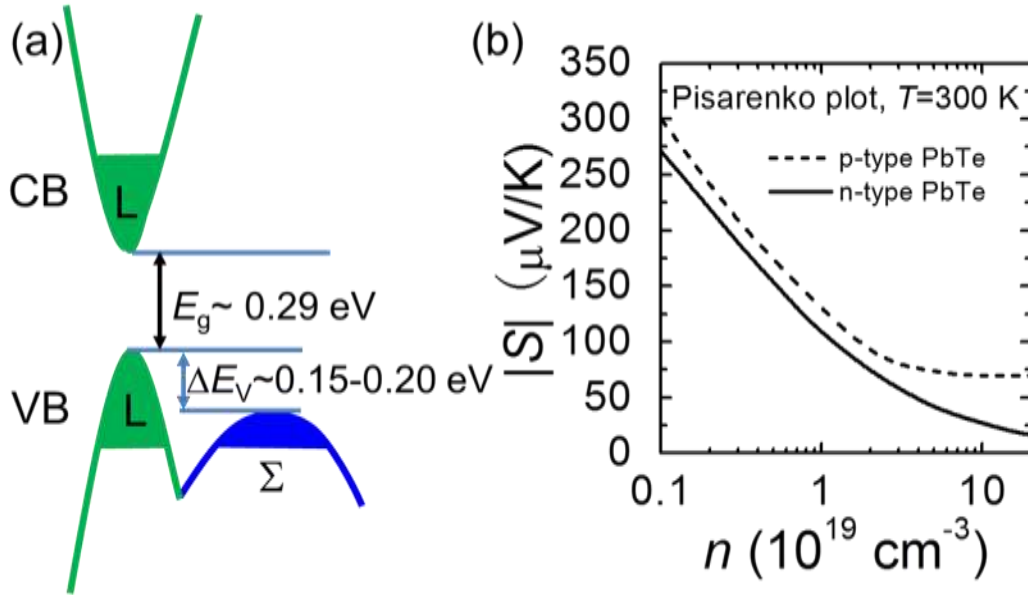


Figure S1. (a) A schematic diagram of the band structure of PbTe.<sup>[1-2]</sup> Both the conduction band (CB) minima and valence band (VB) maxima of PbTe occur at the L points of the Brillouin zone, separated by a direct band gap of  $\sim 0.29$  eV at room temperature. Aside from the primary valence band at L band, there is a second lower-lying valence band with larger effective mass at  $\Sigma$  point. The energy separation of the two valence bands ( $\Delta E_V$ ) is  $\sim 0.15-0.20$  eV at 300 K. (b) The comparison of theoretical Pisarenko plots of n- and p-type PbTe at room temperature.<sup>[3-4]</sup> P-type PbTe has higher absolute Seebeck coefficient than the n-type one, especially at high doping levels ( $n > 2 \times 10^{19} \text{ cm}^{-3}$ ) where the heavy valence band at  $\Sigma$  point is activated.

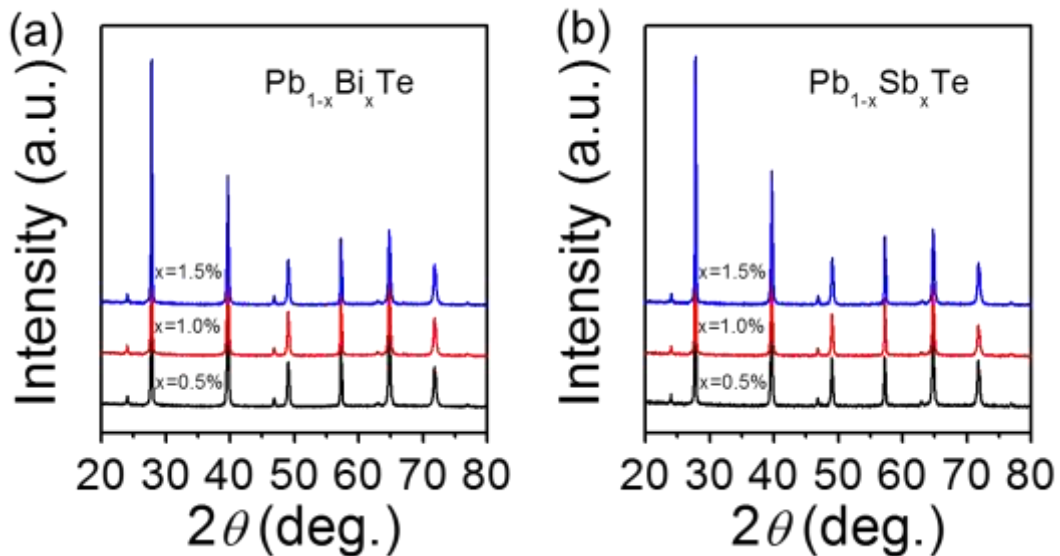


Figure S2. Powder X-ray diffraction patterns of (a)  $\text{Pb}_{1-x}\text{Bi}_x\text{Te}$  and (b)  $\text{Pb}_{1-x}\text{Sb}_x\text{Te}$  with selected compositions.

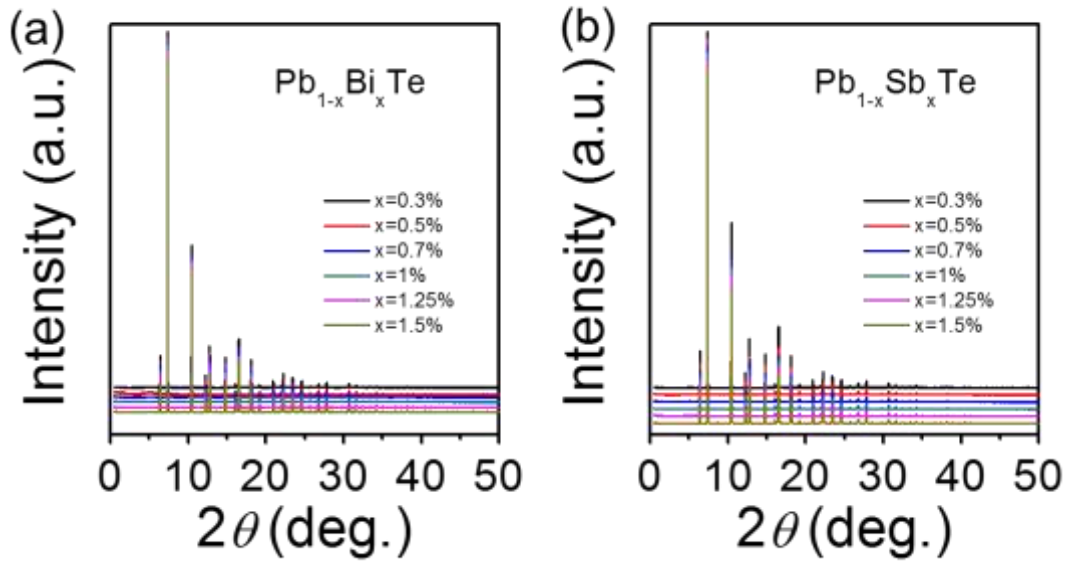


Figure S3. Synchrotron powder XRD patterns for (a)  $\text{Pb}_{1-x}\text{Bi}_x\text{Te}$  and (b)  $\text{Pb}_{1-x}\text{Sb}_x\text{Te}$ .

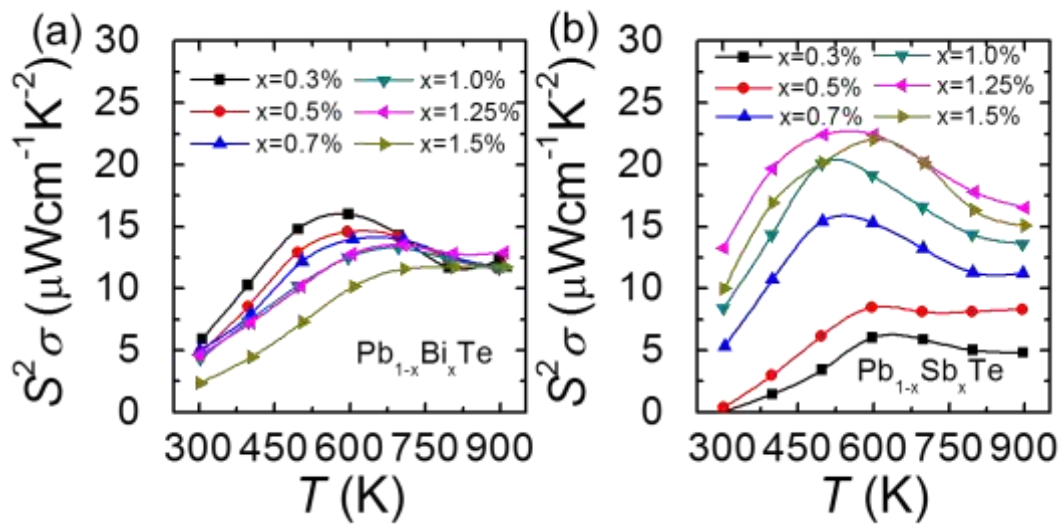


Figure S4. Temperature dependent power factors for (a)  $\text{Pb}_{1-x}\text{Bi}_x\text{Te}$  and (b)  $\text{Pb}_{1-x}\text{Sb}_x\text{Te}$ , respectively.

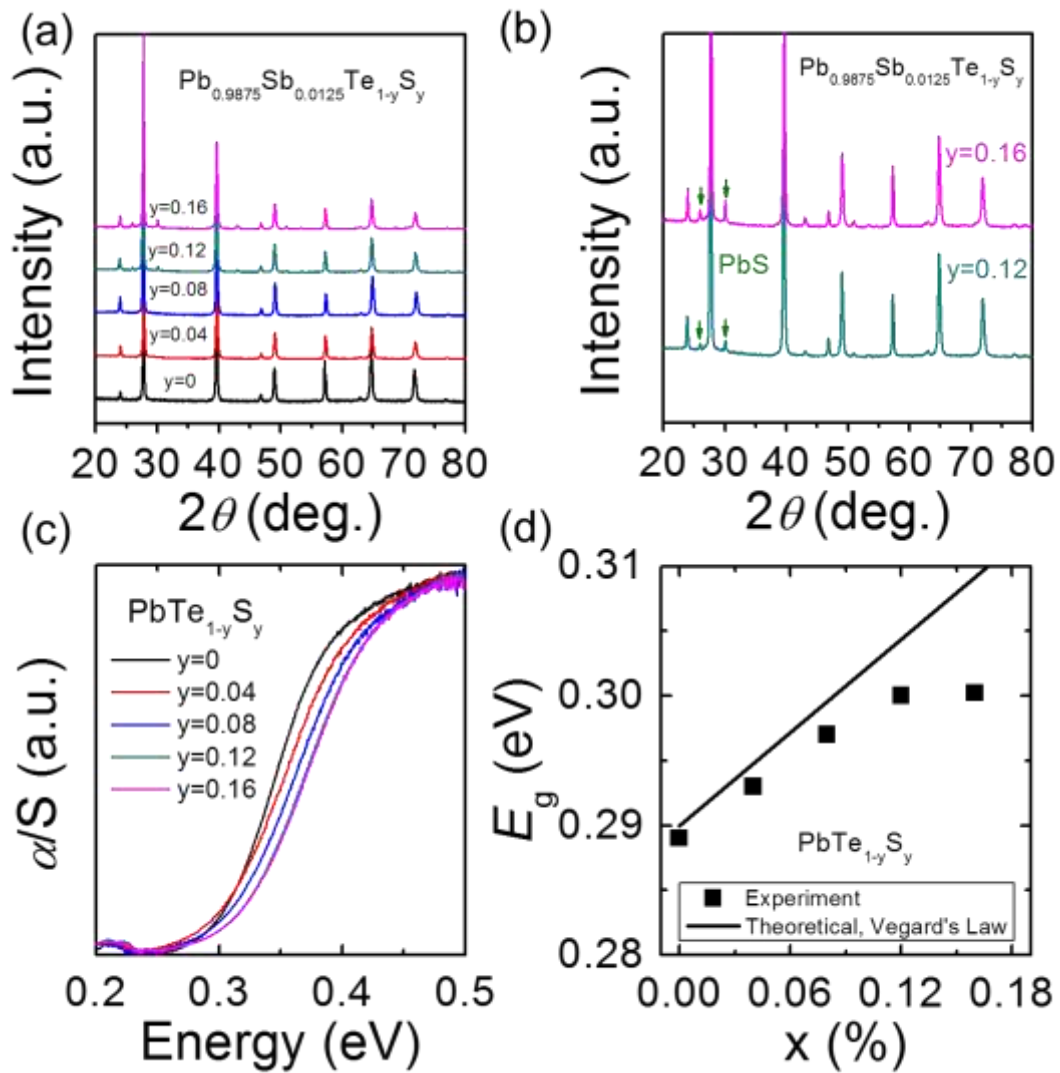


Figure S5. (a) Powder X-ray diffraction patterns for  $\text{Pb}_{0.9875}\text{Sb}_{0.0125}\text{Te}_{1-y}\text{S}_y$ . (b) Impurity phase of PbS is observable in the  $y=0.12$  and  $y=0.16$  samples. (c) Infrared absorption spectra for low carrier concentration  $\text{PbTe}_{1-y}\text{S}_y$  samples. (d) Optical band gaps as a function of S alloying fraction  $y$  in PbTe, which depart from the Vegard's law (solid line) when  $y > 0.04$ .

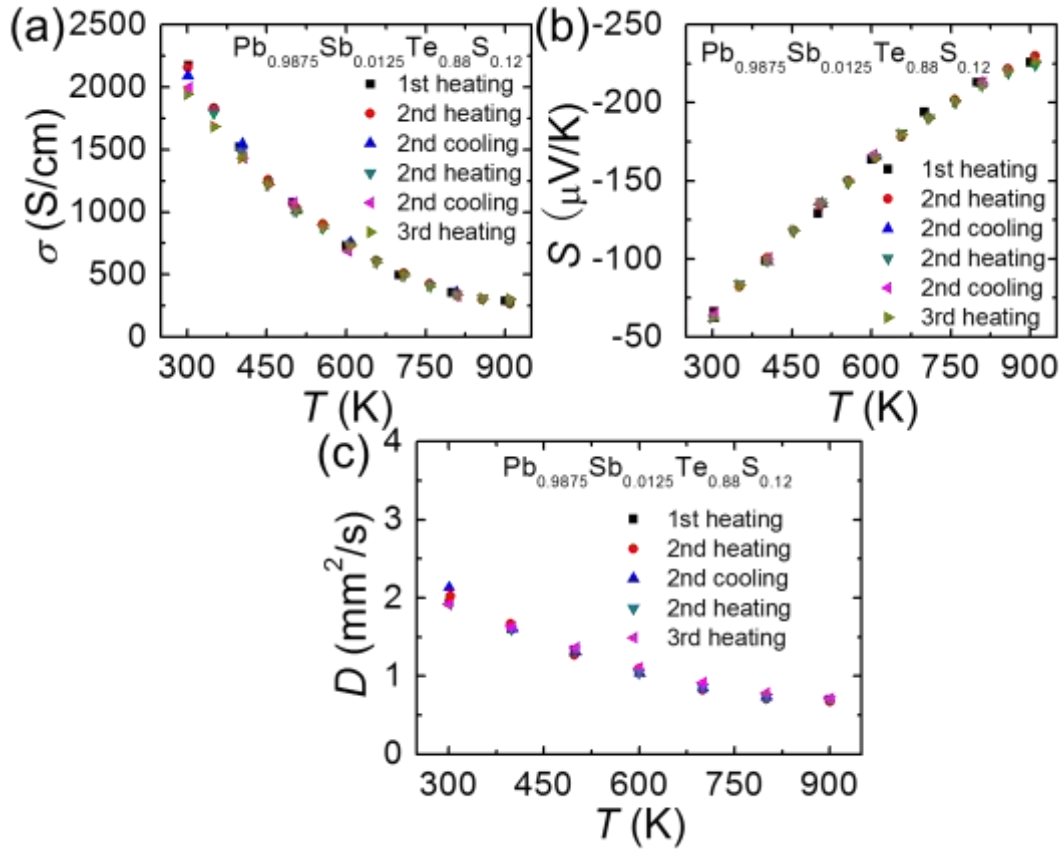


Figure S6. Comparison of thermoelectric properties for  $\text{Pb}_{0.9875}\text{Sb}_{0.0125}\text{Te}_{0.88}\text{S}_{0.12}$  during the first measurement (1st), second measurement with multiple heating-cooling cycles (2nd) and after vacuum annealing at 773 K for 48 hours (3st): (a) Electrical conductivity; (b) Seebeck coefficient and (c) thermal diffusivity.

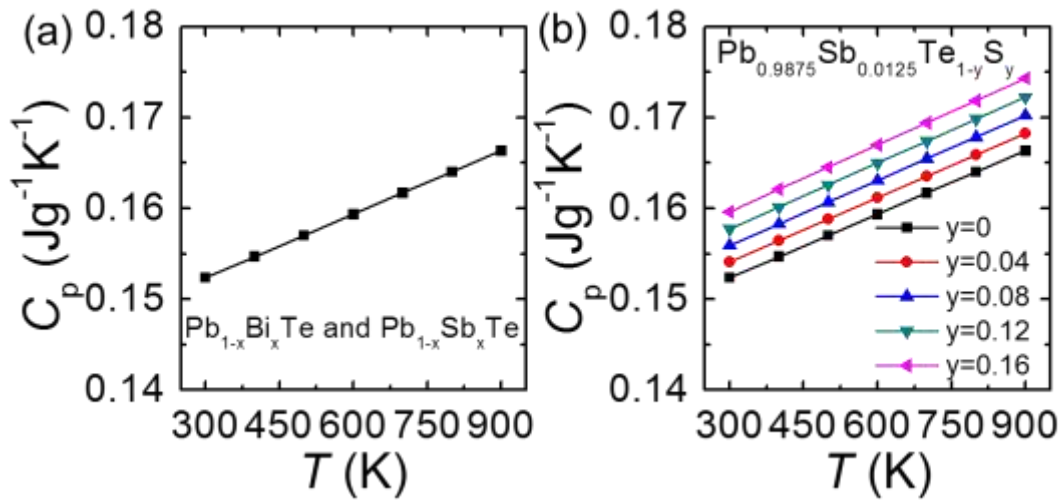


Figure S7. Temperature dependent heat capacities ( $C_p$ ) for (a)  $\text{Pb}_{1-x}\text{M}_x\text{Te}$  ( $\text{M}=\text{Bi}, \text{Sb}$ ) and (b)  $\text{Pb}_{0.9875}\text{Sb}_{0.0125}\text{Te}_{1-y}\text{S}_y$ .

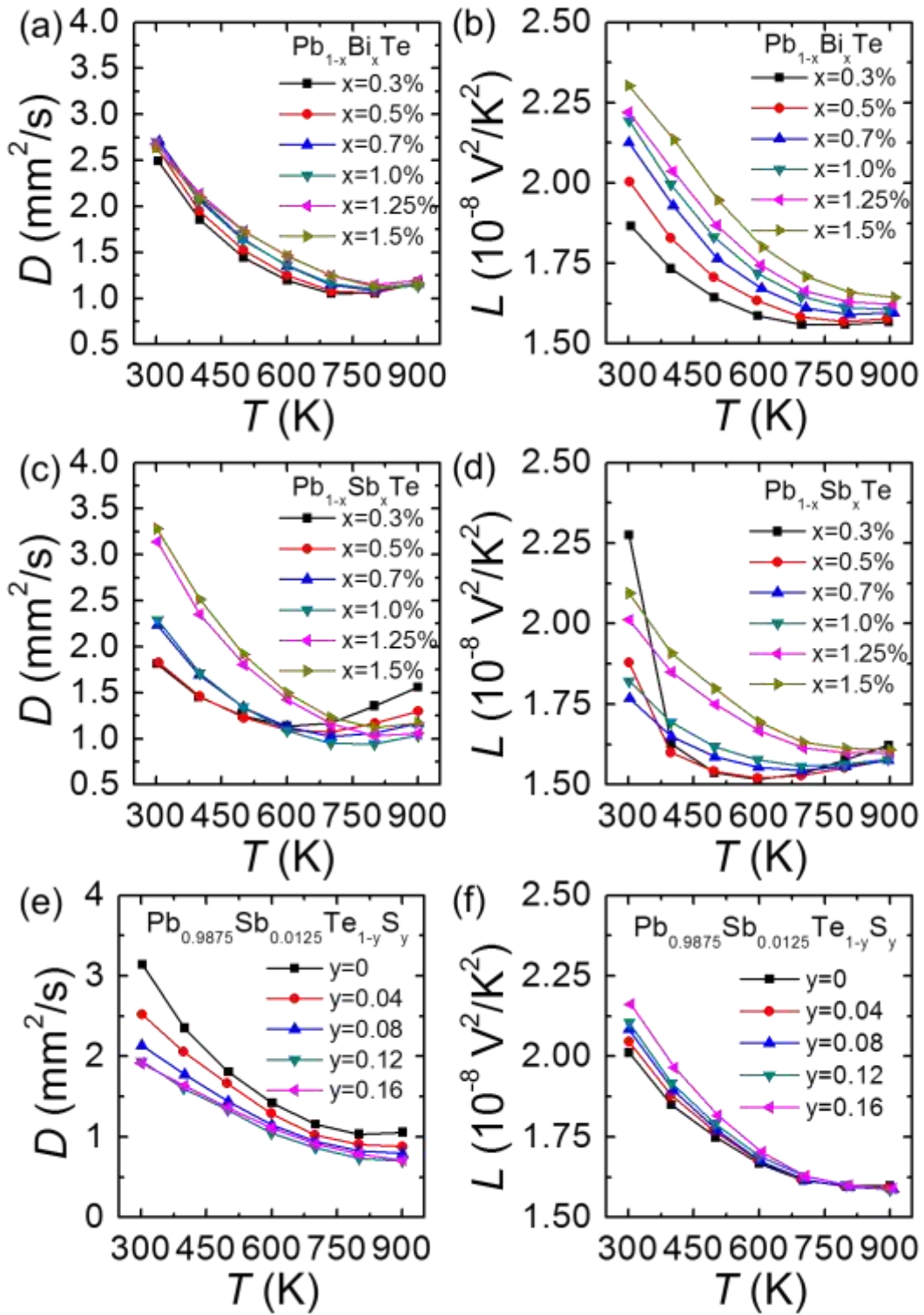


Figure S8. Temperature dependent thermal diffusivities (a, c, e) and Lorenz numbers (b, d, f) for  $\text{Pb}_{1-x}\text{Bi}_x\text{Te}$ ,  $\text{Pb}_{1-x}\text{Sb}_x\text{Te}$  and  $\text{Pb}_{0.9875}\text{Sb}_{0.0125}\text{Te}_{1-y}\text{S}_y$ , respectively.



## Supporting references

- [1] R. Allgaier, B. Houston Jr, *J. Appl. Phys.* **1966**, *37*, 302.
- [2] H. Sitter, K. Lischka, H. Heinrich, *Phys. Rev. B* **1977**, *16*, 680.
- [3] Y. I. Ravich, B. Efimova, V. Tamarchenko, *Phys. Status Solidi B* **1971**, *43*, 11.
- [4] L. Rogers, *Br. J. Appl. Phys.* **1967**, *18*, 1227.